

26

Characterization of Responsive Polymer Brushes at Solid/Liquid Interfaces by Electrochemical Impedance Spectroscopy

Omar Azzaroni and Claudio Gervasi

26.1

Introduction

Characterization of thin and ultrathin polymer films has always attracted great and widespread interest, both for fundamental intellectual and technological challenges, to chemists, materials scientists, physicists, and engineers. This interest stems from their usefulness to a wide range of technological applications that include photolithography, liquid-crystal displays, sensors, or antireflection coatings, among others. Furthermore, as very thin films are incorporated into device applications, it is also necessary to have a better understanding of their physicochemical properties. A more detailed knowledge of the characteristics of polymers deposited on solid substrates is critical for understanding and improving the performance of polymers in numerous applications and is also necessary for further work directed toward the molecular design of soft surfaces. As is well known in the science and technology of surfaces, unraveling and quantifying the physicochemical details of processes occurring within a thin polymer layer is often a challenge. In this regard, impedance spectroscopy is increasingly recognized as a very powerful technique for studying and characterizing thin polymer films deposited on solid supports. Herein, we review some of the basic aspects of electrochemical impedance spectroscopy (EIS) as well as a critical examination of key examples from the literature illustrating its use to investigate polymer brushes. From these examples it is hoped that the reader will get an understanding not only of the information that can be obtained from EIS but also of the way in which this readily available electrochemical technique can open new opportunities to explore the physical properties of surface-confined macromolecular architectures.

26.2

Electrochemical Impedance Spectroscopy—Basic Principles

EIS is a versatile method for probing the features of surface-modified conducting supports [1]. A small-amplitude perturbing sinusoidal voltage signal $\Delta V(t)$ is

applied to the electrode surface, and the resulting current response $\Delta I(t)$ is measured. A quite complex response in the time domain is obtained when the perturbation is not sinusoidal, but of some other function of time t . The response is found as the solution of (a set of) differential equations. A relatively simple method to find a general solution is the method of Laplace transforms. In formal notation, with \mathcal{L} = the Laplace operator and s = the Laplace parameter:

$$\begin{aligned}\Delta V &= \Delta V(t), \quad \mathcal{L}(\Delta V) = \Delta V(s) \\ \Delta I &= \Delta I(t), \quad \mathcal{L}(\Delta I) = \Delta I(s)\end{aligned}$$

For small perturbations, that is, a linear system, the impedance is the ratio of the Laplace transforms of potential and current oscillations with time around the steady-state values;

$$Z(s) = \frac{\Delta V(s)}{\Delta I(s)}$$

With $s = j\omega$ the complex impedance can be written as (Equation 26.1)

$$Z(j\omega) = \frac{\Delta V(j\omega)}{\Delta I(j\omega)} = Z_{\text{re}}(\omega) + jZ_{\text{im}}(\omega) \quad (26.1)$$

where $j = \sqrt{-1}$, $\omega = 2\pi f$ (in radians/second), and f is the excitation frequency (in hertz). The complex impedance can be represented as the sum of the real, $Z_{\text{re}}(\omega)$, and imaginary $Z_{\text{im}}(\omega)$ components that originates from the interfacial relaxation processes.

One approach to model the impedance of the processes taking place at the interface uses circuit analogs or equivalent circuits that describe the experimental impedance spectra. A most popular equivalent circuit is that initially introduced by Randles [2], commonly used to model interfacial phenomena, that includes the ohmic resistance of the electrolyte solution (R_s), the Warburg impedance (Z_W) resulting from the semi-infinite diffusion of electroactive species from the bulk electrolyte to the electrode interface, the double layer capacitance (C_{dl}) and the electron transfer resistance (R_{et}), that represents the charge transfer process of a redox probe at the surface (Figure 26.1).

The parallel connection between the elements C_{dl} and $Z_W + R_{\text{et}}$ indicates that the displacive current (associated with the charging process of the interfacial capacitance on the gold surface) and the faradaic current (due to diffusion and charge transfer of the electroactive species) are considered independent of one

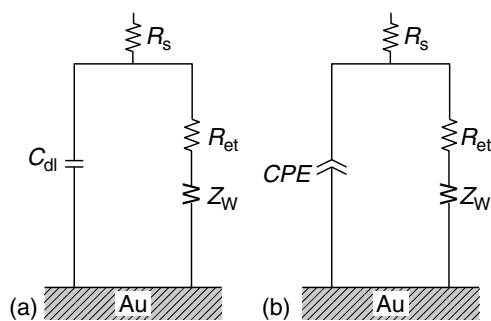


Figure 26.1 Typical Randles equivalent circuit at a gold electrode commonly used in impedance-spectroscopy studies including (a) the double-layer capacitance or (b) a constant phase element (CPE).

another and so the total current through the working interface is the sum of the two distinct contributions [3]. Provided that all of the current must pass through the uncompensated resistance of the electrolyte solution, R_s , is inserted as a series element in the circuit.

Constant-phase elements (CPEs) are used extensively in equivalent electrical circuits for fitting experimental impedance data exhibiting frequency dispersion. The CPE behavior is generally attributed to distributed surface reactivity, surface inhomogeneity, roughness or fractal geometry, electrode porosity, and to current and potential distributions associated with electrode geometry. The frequency dispersion is generally attributed to a “capacitance dispersion” expressed in terms of a CPE.

$$\text{CPE} = A^{-1}(j\omega)^{-n} \quad (26.2)$$

The CPE is represented by two parameters, A and n [3].

A complex-plane representation for impedance data according to the Randles circuit (Nyquist plot) is shown in Figure 26.2. A typical EIS response describes a semicircle region followed by a straight line. The semicircle region (obtained at high frequencies) corresponds to the electron-transfer-limited processes, whereas the straight line with -45° slope (low frequencies) represents semi-infinite linear diffusion or Warburg diffusion. Hence, the electron-transfer kinetics and the diffusional characteristics can be extracted from the EIS data. The semicircle diameter represents R_{et} whereas the intercept of the semicircle with the Z_{re} -axis for $\omega \rightarrow \infty$ corresponds to the solution resistance, R_s .

Even though simple inspection of Nyquist plots for experimental data gives a broad hint of the type of processes taking place at the electrode surface, the computational fitting of the experimental data in accordance to the theoretical impedance of the equivalent circuit allows quantitative values to be obtained for the macroscopic circuit parameters that are related to the interfacial processes.

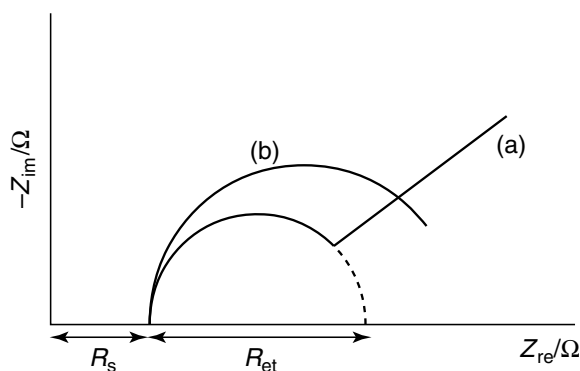


Figure 26.2 Simplified schematic representation of a Nyquist plot describing the impedance spectra of (a) a modified electrode in which the impedance response is governed by diffusion of the redox probe

and the interfacial electron transfer and (b) a modified electrode in which the impedance response is mostly dominated by the interfacial electron-transfer process.

26.3

Electrochemistry as a Tool to Characterize Thin Polymer Films

Electrochemical measurements were employed in the past in highly specialized fields. More recently, this situation has changed quite rapidly, being applied toward interdisciplinary research. The two central aspects of this change are: (i) the use of nonelectrochemical techniques in electrochemical studies (e.g., *in situ* techniques) and (ii) a tendency to use electrochemical tools in numerous scientific fields, with particular emphasis on surface and materials science [4]. Among the different electrochemical techniques, EIS has become particularly valuable to many scientists in the soft-matter community as an alternative characterization method complementing the information achieved using other techniques. EIS has been recently employed to study a wide range of soft-matter-based systems [5], but this chapter will focus on surveying recent progress made in the field of polymer brushes since they represent key building blocks to construct highly functional thin films. Due to the increasing interest from the macromolecular and materials-science community, particular emphasis will be placed on the application of EIS to study their responsive properties under different environmental conditions. When a polyelectrolyte (PE) brush grafted to a conductive surface comes into contact with an electrolyte solution the resulting system acts as a “modified electrode.” Here, EIS serves as a sensitive probe of structural changes in the macromolecular array and provides an initial assessment of brush permeability. Consequently, the technique may be used to characterize not only structural features of the brush but their impact on permeation and reaction of redox probe molecules at the substrate/brush interface, as well. The conformation of the polymer chains in the brush depends strongly on external conditions; especially the ionic strength of the surrounding medium. Thus, conformational changes of the brush may slow down permeability and electrochemical reaction rates. EIS is ideally suited to the study of these steps of the global process in a single experiment, while separating the individual contributions when they exhibit different relaxation time constants.

The typical reaction considered to measure the impedance response of the modified electrode is the reduction of ferricyanide at potentials sufficiently cathodic to allow the anodic reaction to be ignored, yet sufficiently anodic to avoid reduction of oxygen (as a side reaction). Under these conditions, the reaction



provides an example of a first-order reaction involving mass-transfer-limited species undergoing a subsequent charge-transfer step.

The barrier effect of a grafted film or deposited multilayer is usually qualitatively analyzed in terms of the voltammetric response of the bare electrode relative to the response of the film-covered electrode (Figure 26.3). Thus, the voltammogram of the $\text{Fe(CN)}_6^{3-/4-}$ redox system presents a quasireversible behavior at the bare electrode, while the blocking properties of the modified electrode surface bring about a change in shape of the system’s response characterized by an almost

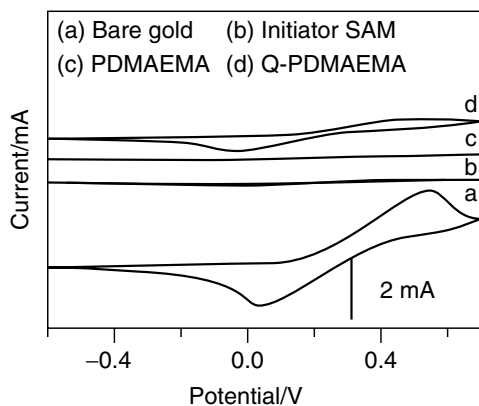


Figure 26.3 Cyclic voltammograms of $\text{Fe}(\text{CN})_6^{3-/4-}$ on different electrodes: bare gold, initiator-modified gold, poly (dimethylamino)ethyl methacrylate (PDMAEMA) functionalized electrode, and a quaternized PDMAEMA brush. Reprinted with permission from Ref. [6] by American Chemical Society.

featureless voltammetric trace with peaks that may become no longer detectable (see Figure 26.3) [6].

In this situation EIS can still be used to obtain quantitative information on the system. If the electron-transfer reaction takes place at bare spots on the electrode surface, the fractional coverage may be estimated by comparing the charge-transfer resistance of the modified surface with the charge-transfer resistance of the substrate surface without modification. If the voltammetric response, although no longer quasireversible, still allows determinations of peak currents, then one may be tempted to calculate the fractional coverage in terms of the ratio of peak currents (I_p) for the bare and covered electrodes. However, it has been demonstrated that this approach is inappropriate for describing the fractional coverage because of the dominance of radial diffusion near each defect site and, as a result, peak currents that are not a simple function of the exposed area [7]. Consequently, values for fractional coverage obtained from impedance spectroscopy data are more reliable. Moreover, the high-frequency measurement of the electrode's impedance, allowing the double-layer capacitance (C_{dl}) to be obtained, is also a fruitful method to follow the percentage of covered surface [8].

Charge-transfer dynamics at the electrochemical interface are strongly influenced by the nature of the electrode surface and the structure of the electrical double layer. Recent studies of electrodes modified by grafted PE brushes have shown that electron transfer to a species in solution is retarded either by reducing the active area of the electrode or by preventing the redox species from approaching the electrode closely [6]. This phenomenon improves the measurement of fast charge-transfer kinetics resulting from a reaction of the type of Equation (26.3) which otherwise is difficult to observe on bare metal electrodes because it is diffusion limited over most of the polarizable range of the electrode. The impedance of an electrode covered with thin permeable polymer films undergoing heterogeneous electron transfer is usually described in terms of an equivalent circuit derived from the model by Randles [9, 10]. Effects of solution resistance, double-layer charging, and currents due to diffusion or to other processes occurring in the surface film can be observed more explicitly using impedance spectroscopy as compared to chronoamperometry and cyclic voltammetry. If the electron-transfer reaction takes place at bare spots on the electrode surface, the fractional coverage may be estimated by comparing

the charge-transfer resistance of the modified surface with the charge-transfer resistance of the surface without modification.

26.4

Probing the Responsive Properties of Polymer Brushes through EIS Measurements

Polymer brushes are increasingly used in many physical systems such as colloid stabilization, polymeric surfactants, polymer compatibilizers, and copolymer microphases [11]. A polymer brush consists of end-tethered polymer chains stretched away from the substrate so that in the given solvent the brush height (h) is large compared to the end-to-end distance of the same nongrafted chains dissolved in the same solvent. In polymer brushes the distance between grafting points (d) is smaller than the chain end-to-end distance. Typically, these systems are characterized by a balance of elastic and excluded-volume interactions. There is also increasing interest in PE brushes, where electrostatic interactions between charges on the polymer and ions in solution play a dominant role. To some extent, PE brushes have been considered as a new class of material provided that strong segment–segment repulsions and the electrostatic interactions bring about completely new physical properties contrasted with noncharged polymer chains. The range of possible electrostatic interactions in PE brushes introduces new opportunities for manipulating the brush structure and its corresponding properties. For example, PEs in solution change from an extended conformation in low ionic strength solutions to a coiled conformation in solutions of high ionic strength. When PEs are covalently attached to a surface to form a PE brush, the polymer chains show a strongly extended (stretched) conformation in pure water, as a result of both repulsion between neighboring chains and repulsion between monomers. Conversely, when polymer brushes are placed in electrolyte solutions, the charges of the pendant groups in the polymer chains are screened, and minimization of the electrostatic repulsions leads to entropically more favorable collapsed conformations. This collapse is comparable to transitions from extended to coil-like conformations commonly observed for PEs in solution. As a result of the constraints on the degrees of freedom related to conformational changes, the PE brush collapse is accompanied by a decrease in film thickness and water content.

In this context, EIS has emerged as a very versatile tool to explore diverse responsive characteristics of PE brushes in different environments. For example, it is well known that poly (N-isopropylacrylamide) (PNIPAM)-based polymers precipitate in water in response to an increase of temperature. Hence, it is reasonable to suppose that the interfacial properties of Au electrodes modified with PNIPAM brushes will display thermocontrolled electrochemical properties [12]. Figure 26.4 describes the variation of the electron-transfer resistance (ETR), as obtained from modeling the impedance response, upon cycling the temperature of the electrolyte solution below and above the lower critical solubility temperature (LCST) of PNIPAM. The low interfacial ETR ($R_{\text{et}} \sim 100 \text{ k}\Omega$) at 25°C reveals that the polymer is in an expanded coil state, whereas the high interfacial ETR

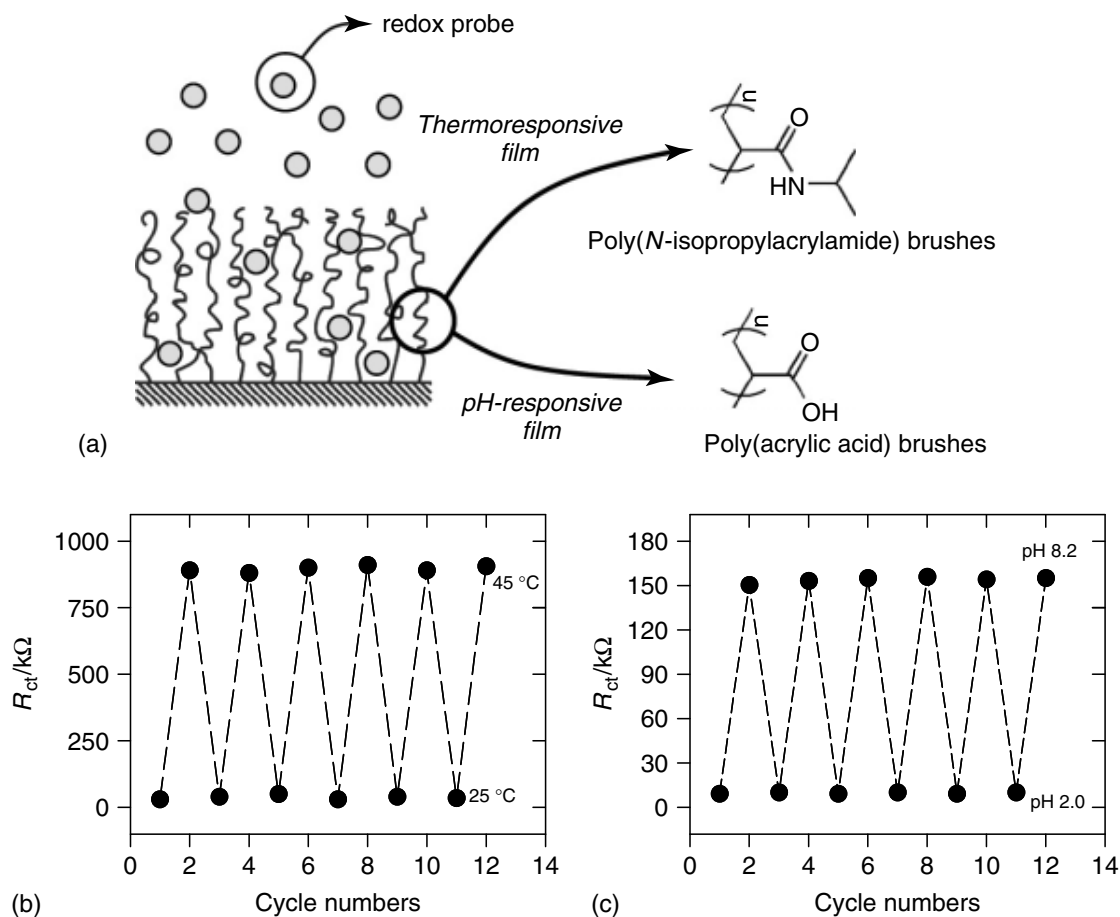


Figure 26.4 (a) Schematic representation of the thermo- and pH-responsive polymer brushes. Interfacial electron-transfer resistance variation upon switching (b) the temperature of PNIPAM-modified Au electrodes and (c) the solution pH of PAA-modified Au electrodes. Reprinted with permission from Ref. [12] by Royal Society of Chemistry.

($R_{et} \sim 890 \text{ k}\Omega$) at 45 °C strongly suggests that the insulating polymer brush is in a collapsed globule conformation. The interfacial ETR shows excellent reversibility, thus indicating that the polymer brushes are very stable. The resulting “ON” and “OFF” cycles of R_{et} can be interpreted by the competition between intermolecular and intramolecular hydrogen bonding below and above the LCST, which controlled the interfacial properties and the permeation of ions or molecules (e.g., $\text{Fe}(\text{CN})_6^{3-/4-}$) through the film. This means that the responsive polymer interfaces are capable of converting environmental information effectively into an electrochemical signal, and this phenomenon may find applications in the construction of “smart” macromolecular platforms.

Grafting polyacrylic acid (PAA) brushes onto conducting substrates may also lead to the facile creation of electrode supports with pH-dependent electron-transport properties. At pH ~ 2 , the R_{et} of $\text{Fe}(\text{CN})_6^{3-/4-}$ is $\sim 1.8 \text{ k}\Omega$. Along with the increase

of pH, the interfacial ETR increased to ~ 160 k Ω (at pH ~ 8). The increase of the interfacial ETR can be attributed to the ionization of carboxylate groups, which enhance the negative charge density of the surface, repelling $\text{Fe}(\text{CN})_6^{3-/4-}$ from the interface. When the pH was repeatedly cycled between 2.0 and 8.2, the variation of R_{et} revealed two well-defined interfacial configurations in which at low pH carboxylate groups are protonated, whereas at high pH the carboxylate groups are fully protonated. In the latter case, the ionic repulsion among COO^- groups in the polymer chain and the anionic redox probes is a key factor setting the high ETR sensed by EIS. Furthermore, the interfacial charge density of PAA brush-modified electrodes can be modulated via changes in the environmental pH, which may lead to novel configurations to manipulate the ion permeability in chemically modified electrodes.

Minko and coworkers [13] described a novel approach to create electrochemical gating systems using polymer brushes grafted to an electrode surface. These authors explored the switchable properties of mixed and homopolymer brushes arising from morphological transitions in the polymer brush layer. The derivatization of indium tin oxide (ITO) electrodes with poly(2-vinyl pyridine) (P2VP) and poly(dimethylsiloxane) (PDMS) brushes enabled the construction of electrode platforms displaying channels formed in the nanostructured thin film in which the precise tuning of their ionic permeability can be manipulated in response to pH changes. In comparison to a homopolymer brush system, the mixed brush showed much broader variation of ion transport through the thin film. Both polymers, P2VP and PDMS, were segregated forming nanosize phases that scale with the mean chain end-to-end distances. Changes in the surrounding environment, such as the quality of the solvent, or pH can promote switching between various phase-segregated morphologies and these structural changes can alter the electrical properties of the brush-modified electrodes.

The EIS spectra of P2VP and P2VP-PDMS-modified ITO electrodes were recorded in the presence of a soluble redox probe, $[\text{Fe}(\text{CN})_6]^{3-/4-}$ in order to monitor the permeability of the polymer brush thin films in different states for the diffusional redox species. The experimentally obtained impedance spectra (Figure 26.5) were fitted by a theoretical equivalent circuit in order to derive the corresponding R_{et} values. This equivalent circuit included the following components: ohmic resistance of the bulk electrolyte solution, R_s , electron-transfer resistance, R_{et} (dependent on the characteristics of polymer brush anchored on the electrode surface), CPE (reflecting the interfacial capacitance distributed in the modifying thin film), and the diffusional Warburg impedance, Z_w (characterizing the diffusional charge transport through the bulk solution) (Figure 26.1b). Of particular importance is the value of R_{et} provided that this parameter obtained at different pHs reflects the various states of the polymer brushes.

The Faradaic impedance spectra of a ITO electrode modified with a P2VP homopolymer brush at different pH values reflects a decrease of R_{et} for the interfacial electron transfer upon acidification of the electrolyte solution.

This interfacial electron transfer originates from the pH-induced swelling of the polymer brush and results in the formation of ion channels. The R_{et} values derived

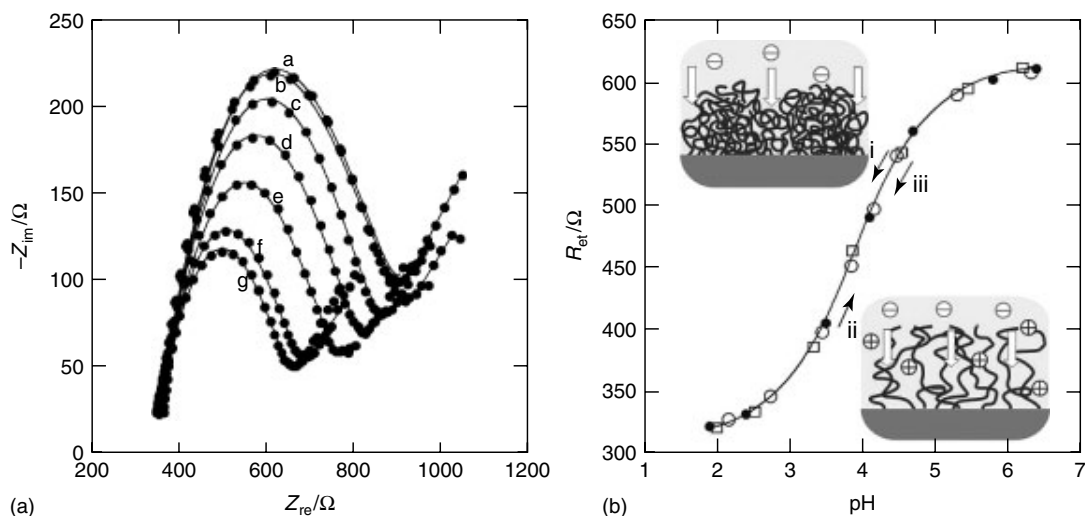


Figure 26.5 (a) Nyquist plot for the impedance measurement of P2VP brush-modified ITO electrodes. (b) Titration curve depicting the changes in R_{et} upon variation of the environmental pH. Reprinted with permission from Ref. [13] by American Chemical Society.

from the fitting with an equivalent circuit of the impedance spectra were plotted as a function of pH to yield a titration curve. This plot eloquently illustrates the structural rearrangements taking place in the polymer brush upon changes in the pH of the solution. The opposite titration (from low to high pH) performed by adding NaOH to the electrolyte solution in the electrochemical cell showed no hysteresis in the pH-induced conformational change of the P2VP brush, that is: the titration curve for the shrinking process of the polymer brush upon increasing the pH value coincides with the titration curve obtained upon acidification of the solution. In this case, EIS provides valuable information regarding the reversible character of the structural changes in the homopolymer brush, which swells and shrinks as the pH decreases and increases, respectively. The open and closed states of the “chemical gate” made of the homopolymer P2VP brush were characterized by variations in R_{et} values between 610 and 320 Ω , respectively.

Similar experiments performed in bicomponent-mixed polymer brush (PDMS/P2VP) also revealed a marked pH-dependent behavior of R_{et} (Figure 26.6). Acidification of the solution causes the electron-transfer resistance values to decrease, thus demonstrating the opening of the “chemical gate” on the electrode support. Thereafter, the electrolyte solution was titrated with NaOH to raise the acidic solution to a neutral pH. The titration curve shows hysteresis with the first titration curve from the first acidification experiment. However, the next acidification cycle repeated the titration curve obtained upon the second “alkaline” titration. All other titration experiments result in the same highly reproducible dependence of R_{et} versus pH. This interesting set of experiments highlights the versatility of EIS as a tool to study the emergence of hysteresis in interfacial processes involving structural changes of polymer brushes. The reorganization

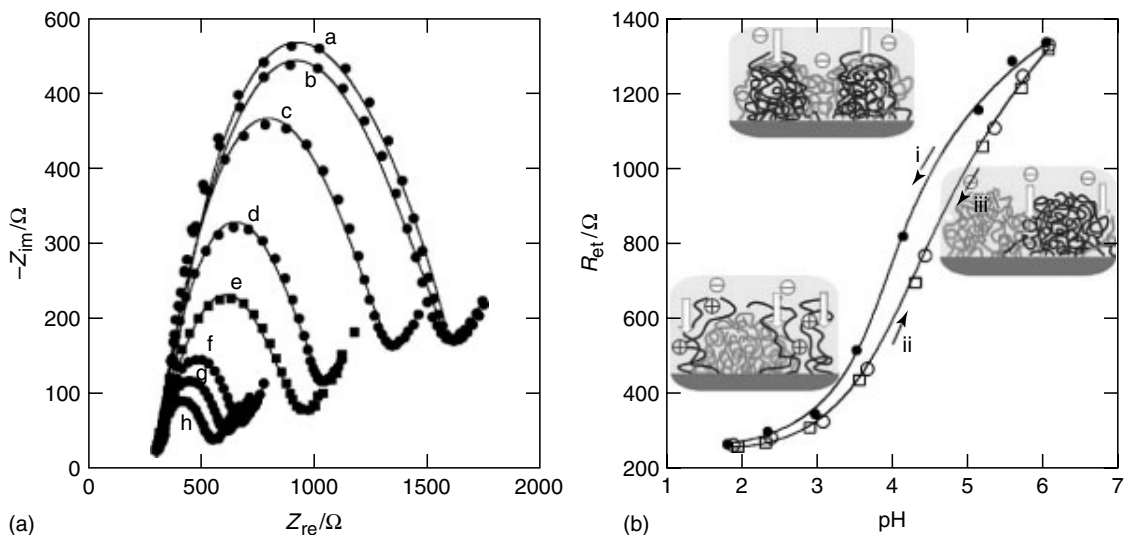


Figure 26.6 (a) Nyquist plot for the impedance measurement of P2VP-PDMS brush-modified ITO electrodes. (b) Titration curve depicting the hysteresis and changes in R_{et} upon variation of the solution pH. Reprinted with permission from Ref. [13] by American Chemical Society.

of the nanostructured polymer brushes upon changes in the pH value results in the reversible shrinking and swelling of the brush that, in turn, is electronically transduced in the closing and opening of the chemical gate on the interface.

These authors also demonstrated that the range R_{ct} changes measured by EIS is significantly larger for the bicomponent-mixed polymer brush compared to the monocomponent brush. Most of this difference corresponds to the closed state of the gate (the maximum value of R_{et} is $\sim 1350 \Omega$ for the mixed brush and $\sim 610 \Omega$ for the monocomponent brush). This was ascribed to the fact that the nonpolar component of the mixed brush contributes to the high electron-transfer resistance in the closed state of the chemical gate, resulting in twofold higher resistance for the interfacial electron transfer compared to that in the monocomponent brush.

In a similar vein, Zhou *et al.* [6] also employed EIS to probe the responsive properties of cationic brushes constituting quaternized poly[(dimethylamino)ethyl methacrylate] (Q-PDMAEMA) tethered onto a gold surface in different electrolytes containing a 1 mM $K_3[Fe(CN)_6]/K_4[Fe(CN)_6]$ (1:1) mixture as a redox probe. Conformational transitions in PE brushes were studied as a function of changes in the electrolyte concentration.

Experimental Nyquist spectra exhibit a single loop in the high-frequency region followed by a straight line with a 45° slope (Warburg-like region) at lower frequencies (Figure 26.7). However, it must be noticed that the lowest frequency of measurement was $\omega = 0.1$ Hz, that is, relatively high. The equivalent circuit shown in Figure 26.2a was used to account for the phenomena that influence the impedance response of the studied system. In turn, this circuit is a derivation from that developed by Jennings and coworkers [14] for pH-responsive copolymer

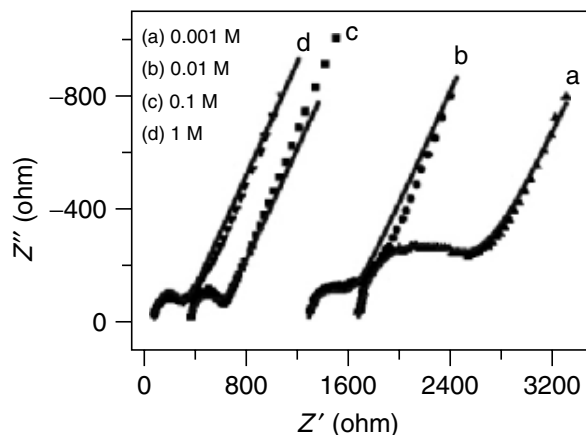


Figure 26.7 Nyquist plots of Q-PDMAEMA brushes at different NaNO_3 concentrations in the presence of 1 mM $[\text{Fe}(\text{CN})_6]^{3-/4-}$ (1 : 1) mixture. In all cases the measured data points are shown as symbols with the calculated fit to the equivalent circuit as a solid line. Reprinted with permission from Ref. [6] by American Chemical Society.

films on gold and shown in Figure 26.8a. The essential difference between the two electrical analogs is the parallel connection between the Warburg impedance and the interfacial capacitance C_i . This modification indicates that, for this, as well as for a second comparable system [15], the current due to interfacial double-layer charging and the faradaic current owing to the electrochemical reaction of the redox probe, are considered to be independent of one another. Surprisingly, the film resistance R_f in series connection with the interfacial impedance is retained, although this resistance results from ionic permeation through a polymeric. Thus, it would have been perhaps more realistic to consider this resistance as an ohmic resistance related to an aqueous electrolytic path inside the brush. Moreover, both relaxation time constants in the model at high frequencies must be similar to account for a single capacitive loop (or two highly overlapped contributions) as shown in the experimental spectra.

On the other hand, it is asserted that in the absence of an electroactive redox species the circuit in Figure 26.8a transforms into the circuit in Figure 26.8b [16]. Thus, for the special case of no redox probes present R_i approaches infinity and thus,

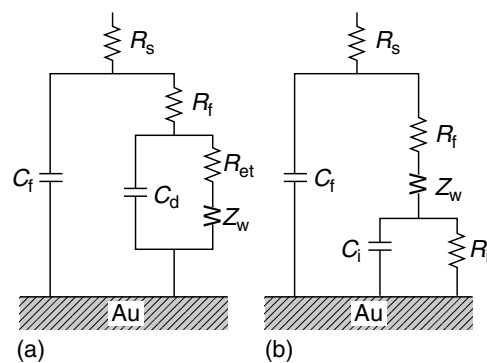


Figure 26.8 Equivalent circuits used to model the impedance spectra of gold electrodes modified with polymer brushes in the presence (a) and in the absence (b) of redox probes in solution.

the interfacial conductance is purely capacitive. The model in Figure 26.8b is used when R_f is much larger than the combined impedance of R_i and C_i in parallel connection, so only the time constant due to the polymer is observed in the impedance spectrum. The Warburg impedance Z_w in Figures 26.8a,b is claimed to be related to ion transport through the film. However, it remains unclear how, for a system that can be modeled with the equivalent circuit Figures 26.8b, diffusional ion transport can be modulated with the applied sinusoidal potential (Warburg impedance element) if the diffusing species is not electroactive (redox species absent).

The difficulties in the analysis described above derive from the use of circuit analogs to model experimental impedance spectra [17, 18]. Consequently, a word of caution must be expressed concerning the use of equivalent-circuit modeling under certain experimental conditions. In order to represent certain processes believed to take place in the system additional elements are usually incorporated in the basic Randles circuit or the type of connection (series or parallel) is altered, expecting to obtain a better agreement between theory and experiment. However, using multicomponent models to fully describe impedance spectra poses a risk, in view of the fact that it becomes increasingly difficult to prove the utility and interpretation of each parameter [19].

Despite some limitations, as described above, a number of interesting observations were made by Zhou *et al.* [6] that were derived from their impedance study. Swelling is associated with fast transport of redox species to the substrate surface, while polymer brushes in collapsed states exhibit hindered transport. Some salts (NaNO_3) cause brush collapse due to charge screening, while others such as those with more hydrophobic anions (ClO_4^- , PF_6^- , and Tf_2N^-) induce brush collapse via solubility changes. The collapsed brushes exhibit intrinsically different resistance as probed with impedance. Charge-screened brushes retain good permeability to electroactive probes. Strongly coordinating hydrophobic anions lead to insoluble brushes, resulting in increased impedance.

26.5

Molecular Transport within Polymer Brushes Studied by EIS

Recently, an approach based on the derivation of the theoretical impedance transfer function to unambiguously describe the impedance response was adopted to characterize gold electrodes modified with poly(methacryloyloxy)-ethyl-trimethyl-ammonium chloride (PMETAC) brushes [20]. Experiments were performed in the presence of $\text{K}_3[\text{Fe}(\text{CN})_6]/\text{K}_4[\text{Fe}(\text{CN})_6]$ (1 : 1) mixture as a redox probe in ClO_4^- solutions with different anion concentrations. Figure 26.9 displays experimental and fitted impedance spectra for gold electrodes modified with a surface-tethered PMETAC brush in ClO_4^- -containing solutions with concentrations of 1 mM KClO_4 , 0.1 M KClO_4 , and 1 M NaClO_4 , respectively. All spectra exhibit a high-frequency capacitive contribution and a distinctive contribution at low frequencies that suggests Warburg-type behavior in the electrolyte with lower concentration, while this contribution becomes related to

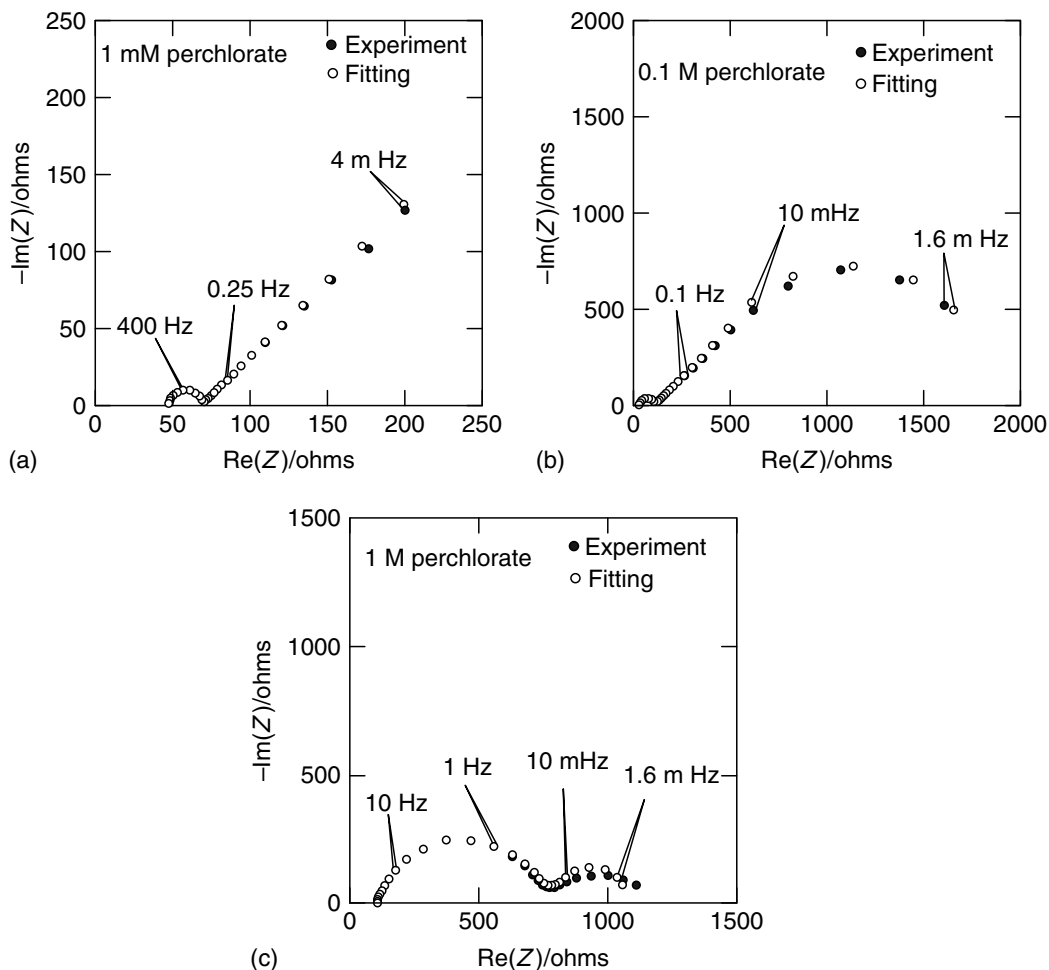


Figure 26.9 Nyquist plots of impedance data for PMETAC-modified electrodes in (a) 1 mM, (b) 0.1 M, and (c) 1 M ClO_4^- a 1 mM $\text{K}_3[\text{Fe}(\text{CN})_6]/\text{K}_4[\text{Fe}(\text{CN})_6]$ (1 : 1) mixture. Experimental data (●) and fittings (○)

according to Equation 26.23 were depicted in the same plots for the sake of comparison. Reprinted with permission from Ref. [20] by American Chemical Society.

finite-length diffusion with an increase in the anion concentration (Figure 26.9). Thus, the high-frequency contribution can be associated with the relaxation of the charge-transfer process at the surface and the charging of the interfacial capacitor, while the second contribution at low frequencies can be related to ionic transport of the electroactive probe through the PE brush.

The increase in impedance values observed for increasing perchlorate concentrations can be ascribed to the ClO_4^- -driven collapse of the PMETAC brush, that may lead to a scenario in which the partial blockage/coverage (θ) of electroactive area is sensitively increased and, as such, the passage of Faradaic current is strongly blocked. It is worth mentioning that the increased blockage is not due to an increase in surface coverage of grafted PE chains at the metal/film interface. The density of anchoring/grafting points of the polymer chains does not change when the brush collapses. The increased blockage results from an increase in film rigidity/density

owing to the strong conformational changes of the polymer chains in the presence of strong ion-pairing interactions. Assuming, as a first approximation, that partial coverage does not affect significantly linear conditions for the mass-transport step at a planar electrode, the effect of the partial coverage is simply to reduce the active area. All impedances are inversely proportional to the active area; thus, if the capacitance of the covered surface can be neglected with respect to the double-layer capacitance of the active surface, all impedance values are inversely proportional to the fractional area of active surface ($1 - \theta$). In particular, these circumstances enable the observed larger charge transfer resistances R_{ct} (Ω) and smaller double layer capacitances C_{dl} (F) for increasing θ , that is, for an increasing degree of collapse of the PE brush to be explained.

Regarding the second time constant at low frequencies, it results from a uniformly accessible electrode to mass transfer through a PE brush of finite thickness. The diffusion impedance response of the brush-containing electrode, when the resistance of the brush to diffusion is much larger than that of the bulk electrolyte, can be approximated by the diffusion impedance of the brush. Moreover, the thickness of the diffusion layer depends significantly on the timescale of a transient experiment, or equivalently on the frequency scale of impedance experiments. If there is a finite length associated with the diffusion layer beyond which the electrode process can have no effect on concentrations, then there is a frequency range for sufficiently low frequencies where impedance response departs from a pure Warburg behavior. Noteworthy, for the experiments shown in Figure 26.9, the lowest measurement frequency was set at a lower value than that used in comparable experiments from the literature [6]. Thus, it can be anticipated that the brush layer represents a diffusion-limiting barrier of finite thickness for electroactive molecular probes (Figure 26.10). Also, when additional negative charges are present in the form supporting electrolyte anions, the diffusion constant of the probe anion is expected to further decrease [21]. In fact, several arguments were advanced in the literature indicating that ion diffusion rather than electron hopping is the charge-transport mechanism in $[\text{Fe}(\text{CN})_6]^{3-}$ -coordinated PMETAC brushes [22].

Figure 26.11 displays experimental and fitted impedance spectra for gold electrodes modified with surface-tethered PMETAC brushes in Cl^- - and NO_3^- -containing solutions with concentrations of 1 M, respectively. Again, when chloride or nitrate replace perchlorate, the impedance response, although exhibiting qualitatively similar dynamics, is quantitatively less affected by the anion concentration, in the 1 mM to 1 M concentration range, as compared to ClO_4^- .

These experimental facts suggest that increasing Cl^- and NO_3^- concentration determines a less-efficient collapse of the brush structure and in turn, the electrode active area becomes less blocked, as compared to perchlorate ion. As previously discussed, the distinctive action of different anionic species in solution originates from ion-pairing interactions between the QA^+ monomer units and the different counterions.

The electrochemical reaction can formally be written as



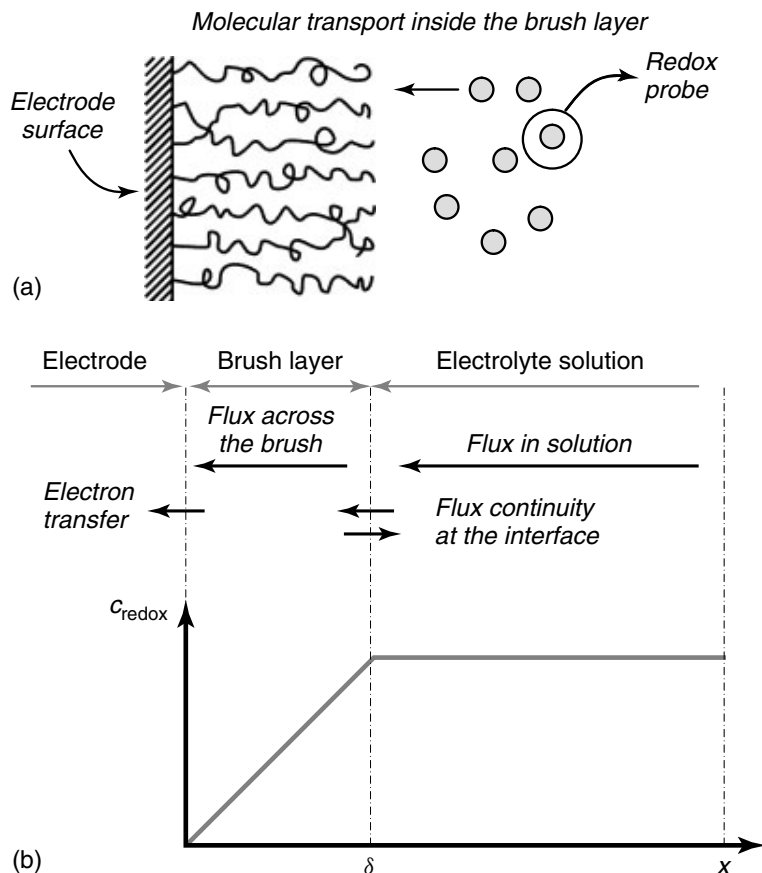


Figure 26.10 (a) Schematic illustration of a gold electrode modified with polymer brushes in the presence of redox probe molecules in solution. (b) Qualitative description of the steady-state concentration profile of redox species under finite-length diffusion conditions (only a concentration profile for the reactive species is considered).

where O is the $[\text{Fe}(\text{CN})_6]^{3-}$ species and R represents the $[\text{Fe}(\text{CN})_6]^{4-}$ species.

The potential (V) dependence of the rate constants can be expressed by an exponential law:

$$k_a = k_a^0 \exp [b_a (V - V_r)] \quad (26.5)$$

$$k_c = k_c^0 \exp [b_c (V - V_r)] \quad (26.6)$$

where $b_c = -\alpha_c F/RT$ and $b_a = \alpha_a F/RT$, k^0 is a constant independent of V , α is the transfer coefficient, and V_r the Nernst equilibrium potential.

Charge balance is given by:

$$I_f = -A_e F [k_c C_O(0) - k_a C_R(0)] \quad (26.7)$$

where $C_O(0)$ and $C_R(0)$ represent concentrations of the oxidized and reduced species at the surface and A_e is the apparent electrode area. The negative sign arises from the assumed convention in which the cathodic current is negative.

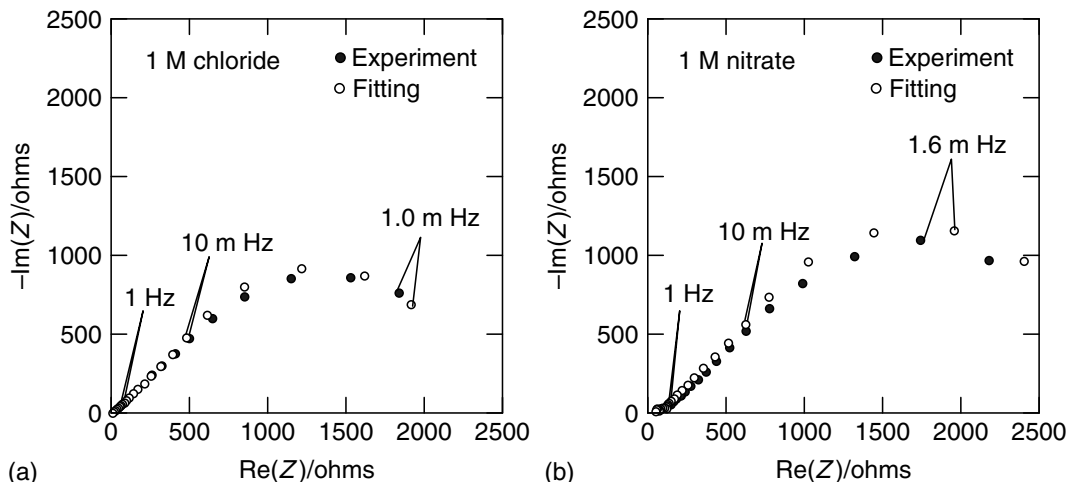


Figure 26.11 Nyquist plots of impedance data for PMETAC-modified electrodes in (a) 1 M KCl and (b) 1 M KNO₃ containing 1 mM K₃[Fe(CN)₆]/K₄[Fe(CN)₆] (1 : 1) mixture. Experimental data (●) and fittings (○)

according Z_f (Equation 26.23), R_s , and C_{dl} , were depicted in the same plots for the sake of comparison. Reprinted with permission from Ref. [20] by American Chemical Society.

When a small ac perturbation signal $\Delta V = \tilde{V} \exp(j\omega t)$ is applied, the current and concentrations oscillate around steady-state values: $I_f = I^{dc} + \Delta I$, $C = C^{dc} + \Delta C$ (for both O and R), where the superscript dc indicates a parameter that changes only slowly with time (i.e. either a steady-state term or one that does not change with the frequency of the perturbation ω), and the symbol Δ indicates a parameter oscillating periodically with time t . The resulting oscillations with time may be written as: $\Delta I = \tilde{I} \exp(j\omega t)$ and $\Delta C = \tilde{C} \exp(j\omega t)$. \tilde{V} and \tilde{I} represent the phasors of potential and current. Taking \tilde{V} as the reference signal and considering the phase shift ϕ between them results $\tilde{E} = E_o$ and $\tilde{I} = I_o \exp(j\phi)$, where E_o and I_o are the amplitudes of the applied potential and the resulting current waves, respectively.

For simplicity, we write a single generic expression for O and R mass balances according the second Fick's law, as:

$$\frac{dC}{dt} = -\nabla J = D \frac{\partial^2 C}{\partial x^2} \quad (26.8)$$

for the flux J along the x coordinate perpendicular to the electrode surface. D refers to the diffusion coefficient of the redox probe.

Or, equivalently,

$$\frac{d\Delta C}{dt} = D \frac{\partial^2 \Delta C}{\partial x^2} \quad (26.9)$$

which in the Fourier domain can be expressed as

$$j\omega \Delta C(x, \omega) = D \frac{d^2 \Delta C(x, \omega)}{dx^2} \quad (26.10)$$

with $j = \sqrt{-1}$

The general solution of the second-order differential (Equation 26.10) is

$$\Delta C(x, \omega) = P \exp\left(x\sqrt{\frac{j\omega}{D}}\right) + Q \exp\left(-x\sqrt{\frac{j\omega}{D}}\right) \quad (26.11)$$

subject, in this case, to the following boundary conditions corresponding to a finite-length diffusion in a system having a transmissive boundary,

$$x = 0 \quad A_e F \Delta J = \Delta I_f \quad (26.12)$$

which expresses the flux continuity condition at the interface, and

$$x = \delta \quad \Delta C = 0 \quad (26.13)$$

which indicates that transfer of electroactive species O and R is possible at $x = \delta$ (thickness of the diffusion layer), while for $x \geq \delta$, C remains unaltered and equal to C^{dc} .

Using Equations 26.11 and 26.13 we can write,

$$\Delta C(0, \omega) = -2Q \exp\left(-\delta\sqrt{\frac{j\omega}{D}}\right) \sinh\left(-\delta\sqrt{\frac{j\omega}{D}}\right) \quad (26.14)$$

and calculate ΔJ at the surface in the Fourier domain

$$\begin{aligned} \Delta J(0, \omega) &= -D \left. \frac{d\Delta C(x, \omega)}{dx} \right|_{x=0} = 2QD\sqrt{\frac{j\omega}{D}} \exp\left(-\delta\sqrt{\frac{j\omega}{D}}\right) \\ &\quad \times \cosh\left(-\delta\sqrt{\frac{j\omega}{D}}\right) \end{aligned} \quad (26.15)$$

Let us call $M(0, \omega)$ the mass-transfer function, defined as [25].

$$M(0, \omega) = \frac{\Delta C(0, \omega)}{\Delta J(0, \omega)}$$

Considering the boundary condition at the surface (Equation 26.12), results

$$M(0, \omega) = \frac{\Delta C(0, \omega)}{\Delta J(0, \omega)} = \frac{A_e F \Delta C(0, \omega)}{\Delta I_f} = \frac{1}{D\sqrt{\frac{j\omega}{D}}} \tanh\left(\delta\sqrt{\frac{j\omega}{D}}\right) \quad (26.16)$$

In order to calculate the reaction impedance Z_f , Equation 26.7 describing the rate of charge transfer should be linearized, according to Taylor-series expansion retaining only terms with first-order derivatives, giving:

$$\begin{aligned} \frac{1}{Z_f} &= \frac{\Delta I_f}{\Delta V} = \left(\frac{\partial I_f}{\partial V}\right)_{\text{dc}} + \left(\frac{\partial I_f}{\partial C_O(0)}\right)_{\text{dc}} \frac{\Delta C_O(0)}{\Delta I_f} \frac{\Delta I_f}{\Delta V} \\ &\quad + \left(\frac{\partial I_f}{\partial C_R(0)}\right)_{\text{dc}} \frac{\Delta C_R(0)}{\Delta I_f} \frac{\Delta I_f}{\Delta V} \end{aligned} \quad (26.17)$$

Derivatives in Equation 26.17 correspond to stationary conditions and may be obtained from Equation 26.7.

$$\left(\frac{\partial I_f}{\partial V}\right)_{\text{dc}} = \frac{1}{R_{\text{ct}}} = A_e F \left[C_O^{\text{dc}}(0) \left(\frac{k_c \alpha_c F}{RT}\right) + C_R^{\text{dc}}(0) \left(\frac{k_a \alpha_a F}{RT}\right) \right] \quad (26.18)$$

$$\left(\frac{\partial I_f}{\partial C_O(0)}\right)_{dc} = -A_e F k_c \quad (26.19)$$

$$\left(\frac{\partial I_f}{\partial C_R(0)}\right)_{dc} = A_e F k_a \quad (26.20)$$

and Equation 26.17 becomes

$$\frac{1}{Z_f} = \frac{1}{R_{ct}} + \left(\frac{\partial I_f}{\partial C_O(0)}\right)_{dc} \frac{M_O(0)}{A_e F} \frac{1}{Z_f} + \left(\frac{\partial I_f}{\partial C_R(0)}\right)_{dc} \frac{M_R(0)}{A_e F} \frac{1}{Z_f} \quad (26.21)$$

For simplicity we assume $D_O = D_R = D$, and so $M_O(0) = M_R(0) = M(0)$ that can be calculated according to Equation 26.16.

Consequently, the reaction impedance can be identified as

$$Z_f = R_{ct} + R_{ct} \frac{(k_c - k_a)}{D \sqrt{\frac{j\omega}{D}}} \tanh\left(\delta \sqrt{\frac{j\omega}{D}}\right) \quad (26.22)$$

which, after rearranging reduces to

$$Z_f = R_{ct} + \frac{\sigma}{\sqrt{\omega}} \tanh\left(B \sqrt{j\omega}\right) (1 - j) \quad (26.23)$$

where the so-called mass transfer coefficient σ contains the contributions of the forms O and R and $B = \delta/\sqrt{D}$.

Finally, the electrode impedance consists of the electrolyte resistance R_s connected in series with a parallel connection of the double-layer capacitance C_{dl} and the reaction impedance Z_f .

Fitting experimental impedance spectra in Figures 26.9 and 26.11 to the theoretical model allows the parameters described in Table 26.1 to be estimated.

Decreasing C_{dl} values (expressed in Farads) were observed for increasing blocking of the active surface area as explained above. A noteworthy fact is that this decrease was also reported in the literature, although it was interpreted in terms of partial exclusion of water from the brush and a decrease in charge density [13]. A most relevant parameter obtained from the fitting procedure is the diffusion coefficient, D , that provides insightful information about the molecular transport of probe species within the macromolecular environment provided by the polymer brush. As a consequence, EIS can be used as a valuable tool to study the effect of different

Table 26.1 Fitting parameters R_s , C_{dl} and those from the reaction impedance Z_f according to Equation 26.23 for the experimental spectra shown in Figures 26.9 and 26.11.

Electrolyte	R_s (ω)	C_{dl} (μF)	R_{ct} (ω)	B ($\text{s}^{1/2}$)	δ (cm)	D ($\text{cm}^2 \text{s}^{-1}$)
KClO ₄ 1 M	1070	8.7	6440	10.47	23×10^{-7}	4.8×10^{-14}
KCl 1 M	8.4	23.6	15.4	13.34	32×10^{-7}	5.75×10^{-14}
KNO ₃ 1 M	53.8	18.0	24	14.4	30×10^{-7}	4.3×10^{-14}

experimental variables, For example: solvent, ionic strength or temperature, on the diffusion of probe species into the brush layer.

26.6

Time-Resolved EIS Measurements on Responsive Polymer Brushes

So far, we have described the use of EIS as a tool to characterize polymer-brush-modified surfaces in a wide frequency range. EIS capabilities can be extended to perform time-resolved experiments to explore, for example, barrier properties of polymer films, that is, considering only relaxation processes exhibiting small time constants. Recently, Jennings and coworkers [23] proposed the use of “single-frequency” measurements as an alternative means to monitor the pH-activated evolution of the barrier properties of copolymer brushes containing polymethylene (99%) with randomly distributed carboxylic groups (1%), PM-COOH. At pH 4, the side chains of PM-COOH were in an uncharged state (-COOH) and the film was hydrophobic due to the prevalence of methylene functionality (99%) along the chains. The film impedance dominates the entire frequency region, indicating that it is much greater than the combined impedance due to the polymer/metal interface (Figure 26.12a). At pH 11, deprotonation of the carboxylic acid side chains increases the hydrophilicity of the film. The increasing charge of the film with pH results in markedly reduced film resistance. While EIS can be used to evaluate the film performance and extract useful properties such as the film resistance and capacitance, each spectrum requires about 10 min to

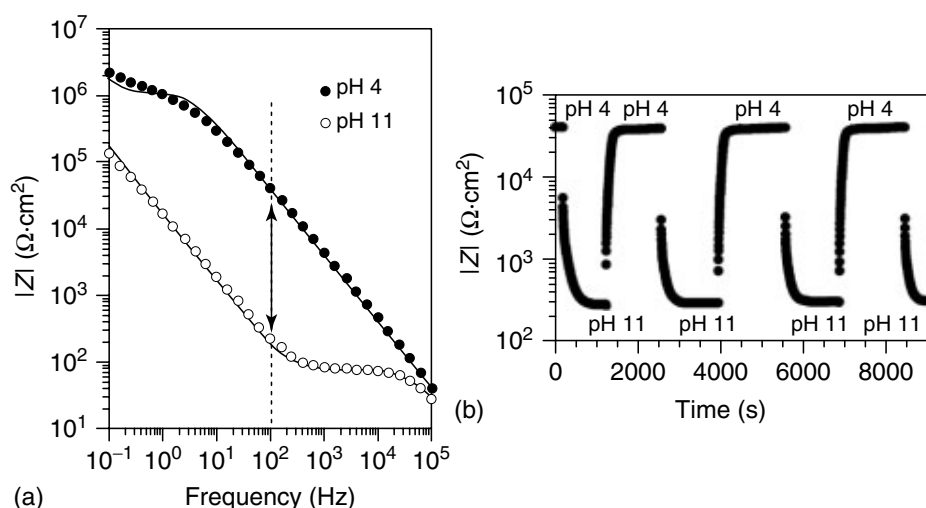


Figure 26.12 (a) Bode plot describing the impedance spectra of PM-COOH brushes with 1% acid content on Au electrodes at pH 4 and 11. (b) Impedance as a function of time when the electrolyte solution is cycled between pH 4 and 11. Reprinted with permission from Ref. [23] by American Chemical Society.

accumulate, precluding a detailed analysis of kinetics on the timescale of several seconds to a few minutes. Consequently, a more rapid sampling method is proposed that consists in evaluating the impedance response at a fixed frequency, after a pH change. Single-frequency measurements can probe the impedance change as a function of time by sampling every few seconds, which enables a more effective monitoring of the rate of film response as the film changes from one state to another. As indicated in Figure 26.12a by the switching of solution pH from 4 to 11, the actual value of impedance modulus is altered by more than 2 orders of magnitude, the largest difference within the studied frequency range. Figure 26.12b shows the measured impedance modulus upon exposure of PM-COOH brushes to pH 4 and 11 buffer solutions in a cyclic manner. The impedance at 100 Hz changes by a factor of 150 when the pH of the contacting solution is switched from 4 to 11. As expected, for each cycle the impedance increases upon exposure to the pH 4 buffer and decrease upon exposure to the pH 11 buffer solution. In this case, single-frequency EIS measurements provide real-time information regarding the response rate and reversibility of the chemical and structural changes taking place inside the brush upon protonation and deprotonation at different pH values.

26.7

Concluding Remarks

We have shown that EIS is a very useful technique to explore, monitor and, more important, quantify the responsive properties of polymer brushes. However, its successful application requires some caution in order to describe a realistic scenario. Worth highlighting is that a good fit of the impedance response is not sufficient measure to validate the proposed scenario. As discussed by Orazem and Tribollet [24], impedance spectroscopy is not a standalone technique. In many cases, additional observations and measurements are needed to validate the suggested physical model. This question is particularly critical when circuit analogs are used to provide quantitative information of the physical processes taking place at the solid/liquid interface in the presence of the polymer film. Consequently, the recommended approach for data analysis and interpretation involves developing a theoretical expression for the impedance in terms of microscopic variables and fitting the experimental results to this model. Within this framework, we consider that EIS may open up new opportunities to characterize the physical properties of polymer brushes as well as the dynamics of their responsive behavior.

Acknowledgments

C.A.G. gratefully acknowledges the Comisión de Investigaciones Científicas y Técnicas Buenos Aires (CICBA) for his position as a member of the Carrera del Investigador Científico. O.A. is a CONICET fellow and acknowledges financial support from the Alexander von Humboldt Stiftung (Germany), the Max Planck

Society (Germany), Agencia Nacional de Promoción Científica y Tecnológica (ANPCyT projects: PRH 2007-74 – PIDRI No. 74, PICT-PRH 163) and the Centro Interdisciplinario de Nanociencia y Nanotecnología (CINN – Argentina). This work was partially funded by UNLP, CONICET, and CICPBA.

References

1. Barsouykov, E. and Mac Donald, J.R. (2005) *Impedance Spectroscopy: Theory, Experiment and Applications*, Wiley-Interscience, New York.
2. Randles, J.E.B. (1947) Kinetics of rapid electrode reactions. *Discuss. Faraday Soc.*, **1**, 11–19.
3. Katz, E. and Willner, I. (2003) Probing biomolecular interactions at conductive and semiconductive surfaces by impedance spectroscopy: routes to impedimetric immunosensors, DNA sensors, and enzyme biosensors. *Electroanalysis*, **15**, 913–947.
4. Rubinstein, I. (ed.) (1995) *Physical Electrochemistry Principles, Methods, and Applications*, Marcel Dekker Inc., New York.
5. Vallejo, A.E. and Gervasi, C.A. (2006) On the use of impedance spectroscopy for studying bilayer lipid membranes in *Advances in Planar Lipid Bilayers and Liposomes*, vol. 3, Chapter 10 (eds H.T. Tien and A. Ottova), Elsevier, Amsterdam, pp. 331–353.
6. Zhou, F., Hu, H., Yu, B., Osborne, V.L., Huck, W.T.S., and Liu, W. (2007) Probing the responsive behavior of polyelectrolyte brushes using electrochemical impedance spectroscopy. *Anal. Chem.*, **79**, 176–182.
7. Finklea, H.O., Snider, D.A., and Fedyk, J. (1993) Characterization of octadecanethiol-coated gold electrodes as microarray electrodes by cyclic voltammetry and ac impedance spectroscopy. *Langmuir*, **9**, 3660–3667.
8. Devos, O., Gabrielli, C., and Tribollet, B. (2006) Simultaneous EIS and in situ microscope observation on a partially blocked electrode application to scale electrodeposition. *Electrochem. Acta*, **51**, 1413–1422.
9. Doblhofer, K. (1980) Electrodes covered with thin, permeable polymer films. *Electrochem. Acta*, **25**, 871–878.
10. Freger, V. and Bason, S. (2007) Characterization of ion transport in thin films using electrochemical impedance spectroscopy. I. Principles and theory. *J. Membr. Sci.*, **302**, 1–9.
11. Advincula, R.C., Brittain, W.J., Caster, K.C., and R  he, J. (2004) *Polymer Brushes: Synthesis, Characterization, Applications*, VCH-Wiley Verlag GmbH, Weinheim.
12. Zhou, J., Wang, G., Hu, J., Lu, X., and Li, J. (2006) Temperature, ionic strength and pH induced electrochemical switching of smart polymer interfaces. *Chem. Commun.*, 4820–4822.
13. Motornov, M., Sheparovych, R., Katz, E., and Minko, S. (2008) Chemical gating with nanostructured responsive polymer brushes: mixed brushes versus homopolymer brushes. *ACS Nano*, **2**, 41–52.
14. Bai, D., Habersberger, B.M., and Jennings, G.K. (2005) pH-responsive copolymer films by surface-catalyzed growth. *J. Am. Chem. Soc.*, **127**, 16486–16493.
15. Yu, B., Zhou, F., Hua, H., Wang, C., and Liu, W. (2007) Synthesis and properties of polymer brushes bearing ionic liquid moieties. *Electrochem. Acta*, **53**, 487–494.
16. Bai, D., Ibrahim, Z., and Jennings, G.K. (2007) pH-responsive random copolymer films with amine side chains. *J. Phys. Chem. C*, **111**, 461–466.
17. Silverman, D.C. (1991) On ambiguities in modeling electrochemical impedance spectra using circuit analogues. *Corrosion*, **47**, 87–89.
18. Harrington, D.A. and van den Driessche, P. (2004) Equivalent circuits for some surface electrochemical

- mechanisms. *J. Electroanal. Chem.*, **567**, 153–166.
19. Raguse, B., Braach-Maksvytis, V., Cornell, B.A., King, L.G., Osman, P.D., Pace, R.J., and Wieczorek, L. (1998) Tethered lipid bilayer membranes: formation and ionic reservoir characterization. *Langmuir*, **14**, 648–659.
 20. Rodríguez Presa, M.J., Gassa, L.M., Azzaroni, O., and Gervasi, C.A. (2009) Estimating diffusion coefficients of probe molecules into polyelectrolyte brushes by electrochemical impedance spectroscopy. *Anal. Chem.*, **81**, 7936–7943.
 21. Reznik, C., Darugar, Q., Wheat, A., Fulghum, T., Advincula, R.C., and Landes, C.F. (2008) Single ion diffusive transport within a poly(styrene sulfonate) polymer brush matrix probed by fluorescence correlation spectroscopy. *J. Phys. Chem. B*, **112**, 10890–10897.
 22. Spruijt, E., Choi, E.-Y., and Huck, W.T.S. (2008) Reversible electrochemical switching of polyelectrolyte brush surface energy using electroactive counterions. *Langmuir*, **24**, 11253–11260.
 23. Bai, D., Hardwick, C.L., Berron, B.J., and Jennings, G.K. (2007) Kinetics of pH response for copolymer films with dilute carboxylate functionality. *J. Phys. Chem. B*, **111**, 11400–11406.
 24. Orazem, M.E. and Tribollet, B. (2008) *Electrochemical Impedance Spectroscopy*, Chapter 23, John Wiley & Sons, Inc., New Jersey.
 25. Jacobson, T. and West, K. (1995) Diffusion impedance in planar, cylindrical and spherical symmetry. *Electrochim. Acta*, **40**, 255–262.